JAAS

Accepted Manuscript

This is an *Accepted Manuscript*, which has been through the Royal Society of Chemistry peer review process and has been accepted for publication.

Accepted Manuscripts are published online shortly after acceptance, before technical editing, formatting and proof reading. Using this free service, authors can make their results available to the community, in citable form, before we publish the edited article. We will replace this *Accepted Manuscript* with the edited and formatted *Advance Article* as soon as it is available.

You can find more information about *Accepted Manuscripts* in the Information for Authors.

Please note that technical editing may introduce minor changes to the text and/or graphics, which may alter content. The journal's standard Terms & Conditions and the Ethical guidelines still apply. In no event shall the Royal Society of Chemistry be held responsible for any errors or omissions in this *Accepted Manuscript* or any consequences arising from the use of any information it contains.

ROYAL SOCIETY OF CHEMISTRY

www.rsc.org/jaas

New Peak Recognition Algorithm for Detection of Ultra Small Nano Particles with Single Particle ICP-MS Using Rapid Time Resolved Data Acquisition on a Sector-Field Mass Spectrometer†

*Jani Tuoriniemi, Geert Cornelis, Martin Hassellöv**

Department of Chemistry and Molecular Biology, University of Gothenburg, SE-412 96

Gothenburg, Sweden

*CORRESPONDING AUTHOR: martin.hassellov@chem.gu.se, tel. +46-31-786 9050, fax +46-31-77227856.

†Electronic supplementary information available

Abstract The applicability of single particle inductively coupled plasma mass spectrometry (spICPMS) is currently limited to particles larger than ~ 10 nm in diameter. In this work the size detection limit (DL_s) was improved by resolving the ion bursts originating from silver or gold nanoparticles (AgNP, AuNP) using real time data acquisition with 0.1 ms time resolution. Such acquisition is here called the Fast Acquisition Speed Technique (FAST). The analytical capabilities of FAST were evaluated on a sector field instrument with high ion transmission efficiency (ITE). An algorithm for distinguishing particle events from dissolved and/or background signal was developed, and it was possible to detect 6.4 nm AuNP that delivered only 2 ions to the detector. The influence of dwell time was investigated and it was concluded that the minimum DL_s is achieved for dwell times close to the duration of the particle events ~ 0.2 ms. Attempts to further improve the DL_s should therefore focus on increasing the ITE of the mass spectrometer.

Introduction

The increasing use of engineered nanoparticles (NP) in consumer products puts both humans and ecosystems at the risk of exposure for these emerging chemicals with poorly assessed health hazards. Accordingly, the concerns have prompted risk assessment and environmental fate studies of NP. Such studies require analytical methods that are capable of distinguishing the NPs from both bulk materials, and dissolved ions, against a complex environmental matrix. Therefore, single particle ICPMS (spICPMS) is currently developed to enable characterization of trace level NP concentrations in environmental and biological samples.[1] The technique has progressed rapidly since the seminal papers by Degueldre *et al*.[2] When NP enters the plasma, they produce bursts of ions with the same yield as dissolved analytes. If the chemical composition of the

particles are known it is possible to calculate their diameters from the intensities of the ion bursts.[3-4] Their number concentration (c_p) can be calculated from their frequency.[3-4] The technique has undergone validation,[5-7] and provided that the nebulization efficiency has been accurately determined, particle diameters can be measured with an uncertainty of a few percent.[5]

Some of the efforts to further improve the technique are directed towards reducing the smallest detectable particle size (DL_s). It is often difficult to distinguish the smallest particle events from fluctuations in the background signal, and therefore, it is in general the noise levels of the dissolved background signal (I_{diss}), rather than the ion transmission efficiency (ITE) of the mass spectrometer that limits the DL_s.[3] The ITE is the fraction of those analyte atoms that enters the plasma, that eventually also reaches the detector. It should be noted that for accurate sizing and measurement of c_p the particle diameters must in general exceed the DL_s with a certain margin.

Therefore, many studies have aimed at reducing the noise levels of I_{diss} by using a Peltier cooled desolvation system and monodisperse droplet introduction,[8] removing dissolved analyte by an ion exchange column,[9] or developing algorithms for deconvolution of the I_{diss} and particle signals (I_{part}).[10] However, determining the sizes of the smallest nanoparticles that only deliver a few ions per particle to the detector would require almost zero noise. This is difficult to reach because of contamination of the instrument and dilution media. Shorter dwell times (t_{dwell}) entail lower intensities, and therefore noise levels of the I_{diss}. However, due to instrument constraints the t_{dwell} in the mentioned studies were considerably longer (> 1 ms) than the duration of the particle events (0.2-0.5 ms).[11] For such acquisition the DL_s is typically limited to about 10 or 20 nm for particles consisting of elements like Ag and Au, for which the DL_s is relatively low.[10] Higher DL_s are found for other nanoparticles.[12]

Obviously, rapid time resolved data acquisition is necessary in order to realize the full potential of spICPMS. Bursts of relatively large particles have been recorded using an oscilloscope connected to the analogue circuit of the electron multiplier detector.[13] However, the current was not amplified sufficiently in their work to detect small fluctuations, and therefore no improvement in DL_s was achieved. Rather, the detector should be operated in the pulse counting mode, acquiring data in real time as a sequence of consequent dwells with t_{dwell} equal or shorter than the duration of the particle events. To be able to in a convenient way distinguish such data acquisition from other approaches, it will be called the Fast Acquisition Speed Technique (FAST) in this article.

FAST was devised for a sector field ICPMS (ICP-SFMS) by Shigeta *et al*.[14] to measure the transient signals from individual droplets formed by a micro droplet generator. ICP-SFMS offers an almost zero dark count rate, and it has the highest ITE among the commercially available instrument designs.[15] The measurement of colloidal nanoparticles by ICP-SFMS was demonstrated by Tuoriniemi *et al.*[5] Since then the analytical capabilities of FAST have been assessed on quadrupole instruments.[16-17] Compared to conventional data acquisition in spICPMS, FAST is capable of characterizing higher particle concentrations, reducing bias due to incomplete

particle events, and make the detector dead time error correction more accurate because the I_{part} fluctuates less during each dwell.[16] However, no improved DL_s was reported because of the poor ITE of the used instruments.[16-17]

Here it is demonstrated that FAST on ICP-SFMS is capable of detecting considerably smaller particles than what has previously been reported. It is important to have systematic means for detection of the particle events. Therefore an algorithm for distinguishing and integrating the particle events is developed, and subjected to a functionality test. The t_{dwell} is a critical parameter for analysis, and it is optimized in this article. For the smallest particles, which only deliver a few ions to the detector, the noise in the particle signals[5] might lead to bias in both size distributions and c_p. The magnitude of such bias as a function of I_{part} is estimated. Finally, the possibilities to further improve the DL_s are discussed.

Experimental

Chemicals

The 40 nm nominal diameter AgNP, and the 5, and 10 nm AuNP were obtained from BBI, UK. These citrate coated particles were diluted between 10^3 to 10^8 times before measurements. The dissolved Ag, In, and Au standards (Ultra Scientific, RI, USA) for spectrometer tuning and calibration were diluted in ultrapure water from 1000 ppm solutions in 2 % HNO_3.

Calibration and particle characterization

The size distributions and number concentrations were calculated as described in references.[3-4] In brief, a calibration curve of signal intensity versus dissolved analyte influx into the plasma is used for calculating the mass of analyte in each particle related peak. The diameters can be calculated provided that the chemical composition of the particles are known, and the ionization and transport efficiencies of the particles are the same as for dissolved analytes. These requirements are fulfilled for the nano-sized particles measured in this work.

In order to know the rate the analyte enters the plasma, it is necessary to measure the nebulization efficiency (f_{neb}), which is the fraction of the sample flow into the nebulizer that manages to enter the plasma. The f_{neb} was determined according to the method by Pace *et al*.[4] The method works by adjusting the f_{neb} during the size distribution calculations, until the measured spICPMS number-average diameter of NIST 60 nm CRM Au particles matched the certified number-average based diameters (Electrospray Scanning Mobility Particle Sizer (ES-SMPS), SEM, and TEM).

Data acquisition

An Element 2 ICP-SFMS from Thermo electron was used in this work. The instrument tune and calibration parameters, and sample introduction components are given in Table 1. The tune parameters were optimized using dissolved In standards. The data was acquired with a time

resolution of 0.1 ms. The reader is referred to Shigeta *et al.*[14] for a comprehensive discussion of FAST using this model of instrument. The following settings were used in the method file of the instrument software to achieve continuous data acquisition with 0.1 ms time resolution: Resolution: *low*, Samples per peak: *1000*, Integration window: *10*. In the low resolution mode ICP-SFMS provides a trapezoidal peak if sensitivity is plotted against mass, with relatively uniform sensitivity over a large part of the mass range covered, but lower sensitivity at very low or very high masses. As the instruments scans through the mass range, 100 consecutive dwells of 0.1 ms t_{dwell} are acquired without any time gap between them. It was confirmed that the masses scanned are within the range of constant sensitivity. The signal is thus monitored continuously for 10 ms, followed by a brief settling time before the next period of FAST. These acquisitions were repeated 3000 – 3500 times in order to monitor the signal during at least 30 s for each sample.

Data analysis

The data was processed in Matlab 7.11 software.

Table 1 Mass spectrometer tune and calibration parameters, and sample introduction components.

Sample gas flow rate (L min^{-1})	Ag ~0.520Au ~0.92
Auxiliary gas flow rate (L min^{-1})	Ag ~0.75 Au ~1.2
Cool gas flow rate (L min^{-1})	Ag ~15.01 Au ~15.9
Sample uptake rate (ml min^{-1})	Ag ~0.48 Au ~0.52
RF power (W)	Ag ~1205 Au ~1000
Nebulizer	Ag, Burgener Mira mist, Au Micromist 0.4 ml/min uptake rate concentric nebulizer (Glass expansion)
Spray chamber	Ag, Cyclonic (Glass expansion) Au, Scott double pass (Glass expansion)
Torch	Fassel type (Thermo Finnigan)
Sample cone	Nickel 1.0 mm orifice diameter
Skimmer cone	Nickel 0.8 mm orifice diameter
Sensitivity[1] (Counts g^{-1})	Ag $4.6*10^{18}$, Au $7.4*10^{\wedge 17}$
Nebulization efficiency	Ag 0.88 %, Au 2.3 %

[1]Sensitivity per mass of analyte introduced to the plasma.

Results and discussion

Particle signals

Fig. 1 shows the particle events produced by the nominally 5, and 10 nm AuNP. They produce an I_{part} having an intensity of not more than a few counts. Signals are shown both for samples in the concentration range of linear response,[3] where particle events can be distinguished from each other, and above the linear concentration range where the particle events have merged into a continuous signal. Fig. 2 shows an ion burst due to a considerably larger AgNP together with illustrations of algorithm parameters. A particle event consists of a peak dwell having the intensity I_{peak}. It is surrounded by a few more dwells on each side having elevated intensity due to I_{part}. Gaussian functions were fitted to 10 AgNP particle events. The standard deviation of the fitted Gaussians, σ_{part} was 0.127±0.024 ms, where the uncertainty is the 95% confidence interval. The r^2 of the Gaussian fit was on average 0.96.Such duration can be regarded as typical for particle related bursts.[11]

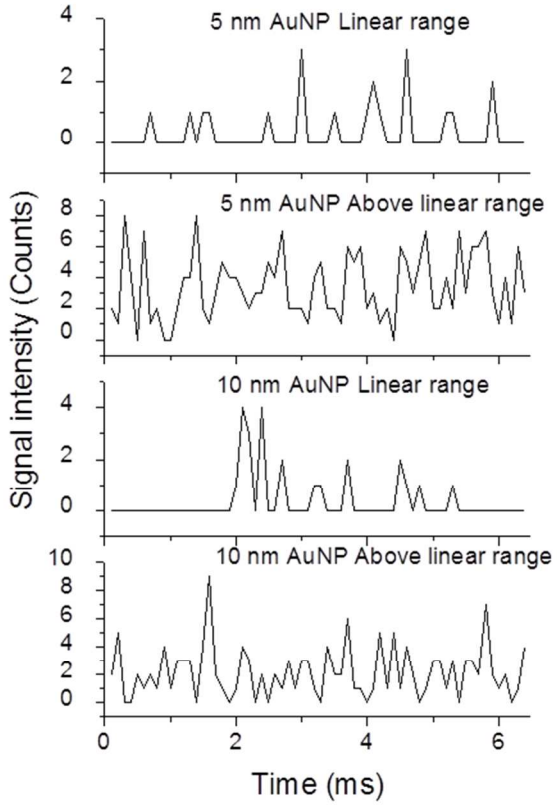

Fig. 1 signals due to the 5, and 10 nm Au particles.

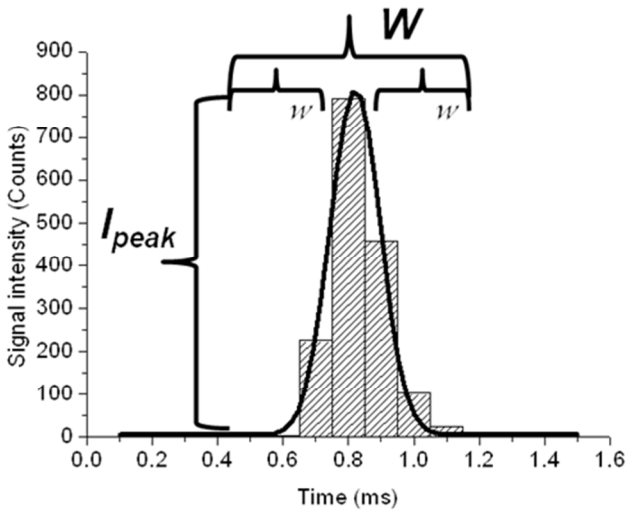

Fig. 2 Signal due to an AgNP acquired with 0.1 ms time resolution. A Gaussian was fitted to the particle event, and it is shown together with the algorithm parameters (The number of dwells on each side of the peak dwell integrated: w=3, and the highest intensity dwell: I_{peak}=820). 16 dwells of 0.1 ms are shown in the graph of which those in the integration windows of width W=2w+1= 7 are integrated as part of the peak.

Particle detection algorithm

Oulier detection Distinguishing the particle events may be based both on the bursts Gaussian shape, and that the I_{peak} is likely to be an outlier in a frequency – intensity diagram. Therefore an existing iterative outlier detection algorithm[3] was modified to suit datasets where the peaks are wider than just a single data point. Criterions concerning the dwells adjacent to the peak dwell were implemented in an attempt to utilize the shape for detection. However this was found to be non-feasible, and was not pursued further in this work. The course of the algorithm is illustrated in Fig. 3. For the most detailed description of the algorithm the reader is referred to the ESI where commented source code, and an additional illustration and discussion are given. The course of the algorithm is as follows.

1) An initial threshold intensity of detection for I_{peak}, $I_{Threshi}$ is set by temporarily removing the 10 % of the dwells that have the highest intensity. This is followed by calculation of the mean intensity, I_i and standard deviation, σ_i of the trimmed data set. Thus a starting threshold is obtained by: $I_{Threshi}= I_i+n*\sigma_i$, where n is an adjustable parameter.

2) The peak dwells of particle events are identified as having both zero crossings in the time-dependent derivative of I (i.e. the difference in signal intensity between adjacent dwells is first positive, and then negative), and an I_{peak} that exceeds the $I_{Threshi}$.

3) The dwells that are within ±*w* (Fig. 2) dwells away from the peak dwell, *i.e.* where zero crossing was identified, are considered to be part of the particle event. They are removed from the dataset until the algorithm has run to completion. A new mean intensity, I_{diss} and a new standard deviation, σ_{diss} of the dissolved signal is computed. In order to facilitate convergence, these parameters are calculated on a trimmed dataset where the dwells with intensities more than three previous standard deviations from their previous mean have been temporarily removed. This way the values of the parameters will more closely reflect the properties of the dissolved signal rather than the remaining particle events. A new lower detection threshold is then calculated as, $I_{Thresh} = I_{diss} + n * \sigma_{diss}$.

4) The steps 2 and 3 are repeated and the detection threshold is successively lowered until no more particle events are detected.

The intensities of the particle signals are calculated by integrating the signal in the ±*w* data points surrounding the peak dwell (Fig. 2). To correct for background, the quantity $I_{diss}*(2w+1)$ is subtracted from the peak area. If a boundary between two continuously acquired sequences of dwells (In this study every 100th dwell) was located within the ±*w* range, the particles are not included in the size distribution; however, they are included in the particle count. This was also done when the ±*w* ranges of two particle events overlap.

Cluster detection At a low average dissolved signal (I_{diss} below ~ 0.5 counts) most dwells will have zero intensity. Particle detection based on outlier analysis works poorly in this case, because any non-zero signal could be regarded as an outlier. Distinguishing of the smallest particle events is instead based on the fact that the ions originating from particles arrive in bursts. Particles delivering 2 ions to the detector will in most cases give rise to the following sequences of dwells 0:2:0, or 0:1:1:0. Particle events of 3 ions would for instance appear as 0:1:2:0, 0:2:1:0, 0:3:0, or 0:1:1:1:0.

It was therefore decided that if the outlier based detection threshold is less than or equal to 2 counts, distinguishing of particle events will instead be based on recognition of clusters of at least *M* ions. *M* has to be set by the user to 2, 3, or 4 in order to reduce the frequency of accidental false positives due to the dissolved signal to an acceptable level. The smallest detectable I_{part} is thus 2 counts, because if only a single ion is detected, it is not possible to determine whether it originated from dissolved or particulate analyte. Even random arrival of dissolved ions at the detector may randomly cause clusters. Dissolved ions may also present some (small degree) of clustering[10] but the expected prevalence of those could be calculated statistically using the model of dissolved signal intensities given in reference.[10] A more detailed description of cluster detection is given in ESI.

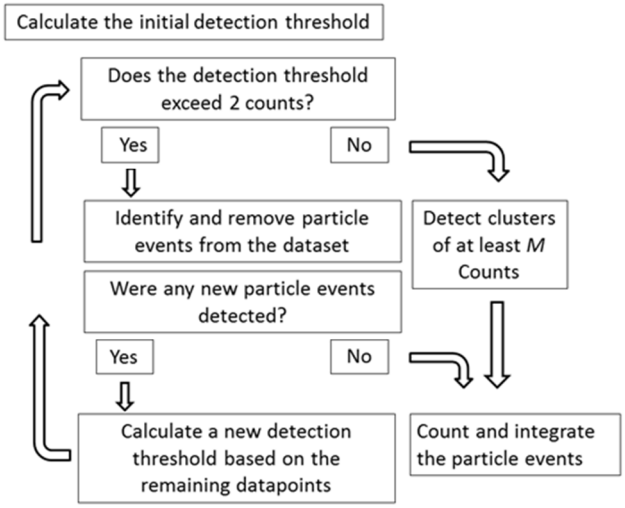

Fig. 3 A diagram illustrating the course of the particle detection algorithm.

The optimization of the algorithm parameters

The adjustable parameters in the developed algorithm are *n, w,* and *M*. They were optimized for minimizing the prevalence of features in I_{diss} becoming falsely identified as particle events, so called false positives; while at the same time not omitting the true particle events from being counted. The samples used for this purpose were the nominally 40 nm AgNP dispersion (106 000 particles mL^{-1}), where the particle events were mostly intense enough (I_{peak} ~ 500-2000 counts) to be easily distinguished from the dissolved background signal; and the 5 and 10 nm AuNP (97700, and 91200 particles mL^{-1}) where the I_{peak} was mostly below 10 counts. Note that for the Ag particles the I_{part} might be large enough for the error due to detector dead time to become significant.[5]

Fig. 4 shows the effect of different values of *n*, *i.e.* the number of standard deviations to be used as a threshold to distinguish background from particle peaks. For values below 3, despite of the significant I_{diss}, the algorithm sets the I_{thresh} close to zero, and there is no discrimination between the signals due to dissolved and particulate analyte. For higher *n* values, the I_{Thresh} increases linearly with *n*. Fig. 4 shows that the particle count remains at a constant value at $n>5$, because no false positives are anymore included in the particle count. Similarly to outlier analysis in conventional spICPMS,[3] an *n* value of 5 can be regarded as a good compromise between keeping the rate of false positives as low as possible, while at the same time not omitting too many true

particle events. The *n* was therefore kept at 5 for the rest of this article.

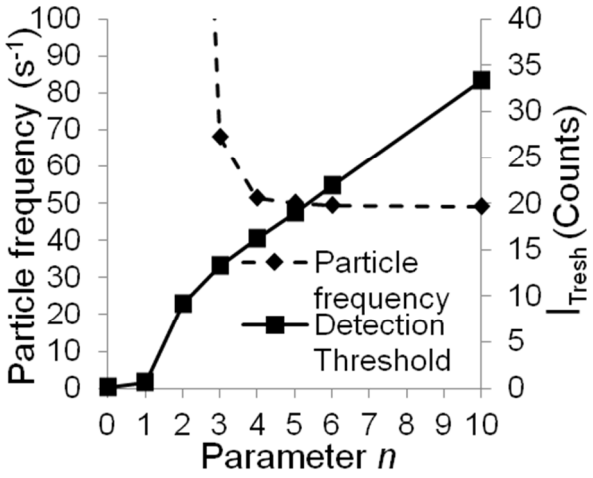

Fig. 4. The particle frequency and I_{Thresh} as a function of the parameter *n*.

For the AuNP the I_{diss} was so low that the algorithm resorted to cluster detection. If cluster detection is used, then the frequency of false positives is determined by the choice of *M*. Higher *M* entails lower frequencies of false positives, but also higher DL_s. If the *M* was set to 2, the spurious particle frequency due to instrument contamination in a blank was ~0.6 particles s^{-1}. This was low enough for true particle events to outnumber the false ones in a broad concentration interval, so *M* was set to 2 in the subsequent experiments with Au particles.

The role of *w* is investigated in Fig. 5. In a gauss curve 99.7% of the values are within $\pm 3*\sigma$ of the average. We can therefore except that *w* should be $\sim 3*\sigma_{part}$ to ensure that the particle events are completely integrated, while at the same time maintaining proper distinction between the particulate and dissolved signals. The integral of the I_{part} is relatively robust with respect to the choice of *w*, as long as the integration window is wide enough to include the whole particle event. The *w* was set to 3 for the rest of this paper, because it is in most cases enough to include all of ions in the particle event. The 40 nm Ag particles seem to be less robust than the Au particles. This is because they are the largest particles therefore forming the largest clouds. A wider part of the tail of the particle event will thus produce a measurable signal. It should be noted that there are also notable differences in burst duration between different elements.[11] The duration of ion bursts seems not to be any simple function of the ion diffusion coefficient in the plasma, and the reasons for the differences are currently not completely understood.[11] Setting *w* too small misses a significant bit of the tails of the Gauss curve, while setting it too high "dilutes" the peak with more background, making it less clear again.

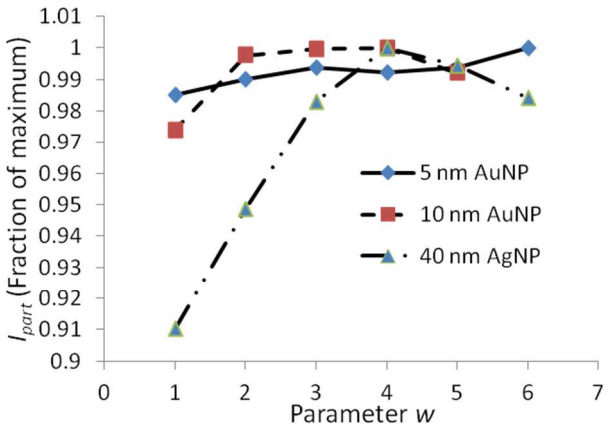

Fig. 5 The particle signal as a function of *w*. The I_{part} for each sample is shown as a fraction of its maximum value in these datasets.

Linear concentration range and size detection limits

In Fig. 6 it is demonstrated that the number of 40 nm Ag (n=5, w=3), and 10 and 5 nm Au particles that are detected with the algorithm (M=2, w=3) increase linearly with concentration (i.e. measured/expected concentration has zero slope as a function of expected concentration). Due to partial dissolution, the samples of 40 nm AgNP contain a significant concentration dissolved analyte that increases as the colloid becomes less diluted. This may obscure the smallest particles from detection, but on the other hand it may produce false positives as well. The result is the notable scattering among the datapoints. Linear response for the AgNP is achieved from concentrations where true particle events dominate over the false positives, to where particle events occur so frequently (> 500 Particles s^{-1}) that the ion bursts frequently overlap making it difficult to distinguish between one larger, or two or more smaller particles arriving close together (Fig. 6). The DL_s was set by the noise levels of the I_{diss}, and it increased from ~ 6 to 15 nm within the linear range.

The detection of AuNP was based on detection of clusters of 2 or more ions. Linear response could be achieved from concentrations where the frequency of true particles events outnumbered the randomly occurring clusters of the I_{diss} (Fig. 6), to where the ion bursts began to merge with the increasing I_{diss} into a continuous signal (Fig. 1). The ITE limited DL_s of 6.4 nm was reached in the whole linear range.

The size distributions of the AuNP are shown in Figure 7 (9770 and 9120 particles mL^{-1} for the 5, and 10 nm AuNP). Note that the apparent modal diameter of the nominally 5 nm particles is ~7 nm. The mean diameter specified by the manufacturer is 5.5 nm, wherefore despite that the particles are not necessarily perfectly spherical; one could expect the concentration to increase with decreasing size until the DL_s. This is because the concentrations of small particles that produce an I_{part} of only a few counts are underestimated, because due to noise particles are not always producing the expected number of ions, and the smallest particles are therefore at the risk

of escaping detection. Furthermore, not every burst of detectable size is such that it is recognized as a particle event by the algorithm. This matter is discussed in detail in ESI. Calculations presented in ESI indicate that only ~ 30 % of the Au particles at DL_s (6.4 nm that produce on average 2 counts) are detected and become counted as particle events. Measurements are fully reliable with respect to this type of bias only if the I_{part}> 10 ions. The c_p of AuNP reported here are however without any corrections for bias.

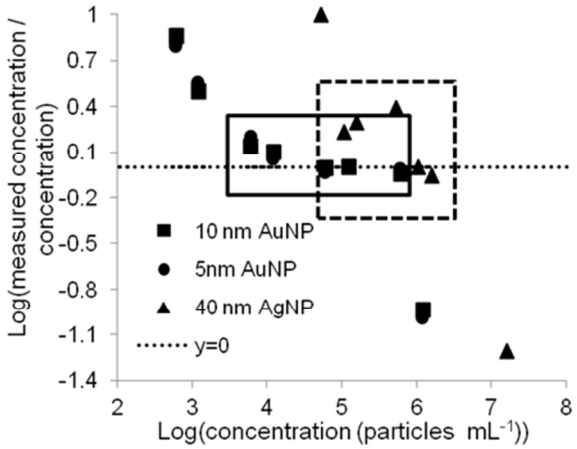

Fig. 6 The logarithm of the particle frequency divided by the number concentration, shown as a function of the logarithm of the number concentration of particles. The linear ranges of 5 and 10 nm AuNP are indicated by the solid line, and the 40 nm AgNP by the dashed line box.

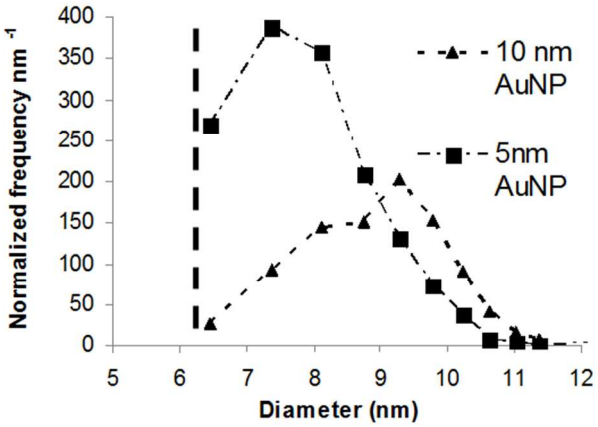

Fig. 7 The size distributions of the 5 and 10 nm AuNP measured by FAST. The vertical dashed line indicates the DL_s.

Effect of t_{dwell} on size detection limits

As long as the whole particle event occurs within one dwell, the ratio of I_{part} to σ_{diss} increases, and therefore DL_s decreases with shorter t_{dwell}.[3] In conventional spICPMS the choice of t_{dwell} is a

tradeoff between obtaining as low DL_s as possible, and minimizing the frequency of incomplete particle events. In FAST spICPMS where the t_{dwell} is shorter than the duration of the particle events, the situation is also complex, because now I_{peak} will also decrease as the dwells become shorter, because a smaller fraction of the particle event is measured during the peak dwell. The particle events may become more difficult to distinguish if the I_{peak} decreases more rapidly as a function of the decreasing t_{dwell} than the σ_{diss}. For a given I_{diss} and ITE of an instrument, there is thus an optimum t_{dwell} having the lowest possible *DLs.* To aid the further development of FAST spICPMS, a model was developed for calculating the optimum t_{dwell}.

For the particle event to be detected, the I_{peak} must be n times higher than σ_{diss}. The σ_{diss} as a function of the I_{diss} can be modeled by the following equation:[10]

$$\sqrt{\beta I_{diss} + c_{fl}^2 I_{diss}^2} = \sigma_{diss} \quad (1)$$

The parameter β gives the magnitude of the shot noise due to random fluctuations in the ion flux. It assumes the value 1 in the ideal case of ions arriving completely randomly at the detector. The c_{fl} is the flicker factor that takes into account noise due to fluctuations in plasma properties, and in the flux and size distribution of the droplets emerging from the spray chamber. The parameters β, and c_{fl} were determined to 1.47 and 0.094 respectively by fitting Eqn (1) to the noise levels in dissolved Ag standards (0.1, 1, and 2 ppb, r^2=1.00).

The criteria for detection can therefore be stated:

$$I_{peak} > n\sqrt{\beta I_{diss} + c_{fl}^2 I_{diss}^2} \quad (2)$$

If the particle event is assumed to have its peak at the center of a dwell, the I_{peak} can be obtained by integrating the Gaussian ion burst centered at $t=0$ between $\pm 1/2\ t_{dwell}$. It results in:

$$I_{peak} = \frac{M_{part} s}{\sigma_{part}\sqrt{2\pi}} \times \int_{-\frac{1}{2}t_{dwell}}^{\frac{1}{2}t_{dwell}} e^{\frac{-t^2}{2\sigma_{part}^2}} dt \quad (3)$$

Where the M_{part} is the mass of analyte in the particle, and s is the sensitivity defined as counts per mass of analyte entering the plasma. The dissolved signal intensity is given by:[3]

$$I_{diss} = t_{dwell} q f_{neb} c_{ion} s \quad (4)$$

where q is the flow rate into the nebulizer, and c_{ion} the mass concentration of dissolved analyte. Combining Eqns 2-4 therefore gives an expression for the smallest detectable mass of analyte in a particle, M_{min} as a function of t_{dwell} and c_{ion}.

$$M_{min}=\frac{n\sigma_{part}\sqrt{2\pi}}{s}\times\frac{\sqrt{\beta t_{dwell}qf_{neb}c_{ion}s+c_{fl}^2{t_{dwell}}^2q^2f_{neb}^2c_{ion}^2s^2}}{\int_{-\frac{1}{2}t_{dwell}}^{\frac{1}{2}t_{dwell}}e^{\frac{-t^2}{2\sigma_{part}^2}}dt} \quad (5)$$

The results produced by Eqn (5) are only meaningful as long as the I_{peak} of the smallest detectable particle is equal to, or larger than 3, because otherwise the algorithm will resort to cluster detection. In Fig. ESI-4 it is confirmed that for a given c_{ion}, the DL_s predicted by Eqn (5) agree with values that were actually determined by the algorithm in samples containing both dissolved and particulate analyte.

In Fig. 8 the M_{min} calculated from Eqn (5) and the experimental values determined by the algorithm (40 nm AgNP, 15 900 particles mL^{-1}, containing 1.6*10^{-10} g mL^{-1} dissolved Ag), is shown as a function of t_{dwell}. The datasets for the experimental values of t_{dwell} > 0.1 ms were created by binning together adjacent 0.1 ms dwells. This procedure guarantees that the underlying signal is equal for all t_{dwell}. Both the calculated and experimental data show that the M_{min} decreases with t_{dwell} as long as the dwells are longer or comparable in duration with the particle events. Reducing the t_{dwell} further from its optimum value of ~0.2 ms results instead in an increasing M_{min}. Note that the difference between the experimental and the calculated values increase with t_{dwell}. This is because as the DL_s increases, the smallest particle events become increasingly classified as background signal. These particle events then cause the apparent σ_{diss} to be higher than what could be predicted from Eqn (1).

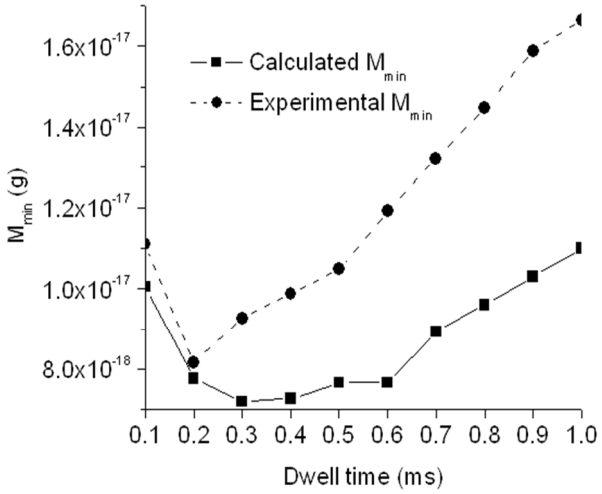

Fig. 8 The M_{min} as a function of t_{dwell} calculated from Eqn (5) and determined experimentally by the algorithm.

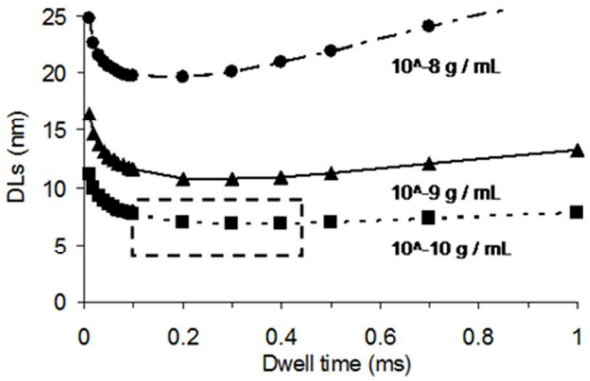

Fig. 9 The smallest detectable Ag particle diameter as a function of dwell time, and dissolved analyte concentration calculated from Eqn (5).The dashed line box indicates where the detection limit is set low enough for cluster detection to be employed. As is discussed in the text, but not indicated in the figure, the algorithm resorts to cluster detection at very short t_{dwell} for all I_{diss}.

In Fig. 9 the Eqn (5) was used for calculating the DL_s as a function of t_{dwell} for a range of dissolved Ag concentrations. The optimal dwell time decreases only little with concentration (From ~ 0.3 ms to 0.2 ms) when the dissolved Ag concentration increase from 10^{-10} to 10^{-8} g mL^{-1}. The DL_s increase sharply for $t_{dwell} < 0.1$ ms. This happens because a given I_{part} is divided among an increasing number of dwells, causing the I_{peak} to decrease faster than the I_{diss}. Meanwhile, the decreasing number of background ions collected per dwell will cause the algorithm to switch to cluster detection for t_{dwell} below 7 µs for 10^{-10} g mL^{-1} and 70 ns for 10^{-8} g mL^{-1}. However, such short t_{dwell} are not likely to improve the DL_s for cluster detection either, because setting $t_{dwell} < \sigma_{part}$ is for small particles only likely to introduce dwells with zero intensity during the particle event.

Conclusions and outlook

An algorithm for quantifying particle events in spICPMS data acquired with FAST was evaluated. It was found to perform satisfactorily for both a significant, and nearly zero dissolved background signal intensities. The FAST allowed pushing the DL_s to the ITE limited value of a sensitive ICP-SFMS instrument, and made it possible to detect smaller particles than what had previously been reported.

It was concluded that further improvements in size detection limit cannot be achieved by only reducing the dwell time from the 0.1 ms used here. The development should rather focus on improving the ion transmission efficiency of the mass spectrometer. For the instrument used in this work only 0.082 % of the Ag and 0.024 % of the Au ions entering the plasma were detected. However, considerably smaller particles could be detected if the ITE was improved. For instance, a 1 nm Ag particle already delivers 31 atoms to the plasma, which would likely be detectable if the ITE could be improved to around 10%.

It is possible to improve the ITE to more than 1 % if the jet sampler cone by Thermo is combined with a high efficiency interface pump, and an aerosol desolvation system.[18] The I_{diss} is proportional to the rate the sample is introduced to the plasma. Combining such high performance sample introduction and interface system with the low sample introduction rates, on the order of $\mu L\ min^{-1}$, that can be attained using micro flow nebulizers, would therefore create a very powerful analytical system for the smallest particles.

Acknowledgements

We would like to thank Dr. Conny Haraldsson (SP, Borås, Sweden) for providing access to an additional, identical mass spectrometer. The research was funded by the FP 7 projects MARINA (CP-FP 263215), Nanofate (CP-FP 247739), and the Nordic Council of ministers (project 1397).

References

1. F. Laborda, E. Bolea, J. Jimenez-Lamana, *Anal. Chem.*, 2014, **86**, 2270-2278.
2. C. Degueldre, P.Y. Favarger, S. Wold, *Anal. Chim. Acta*, 2006, **555**, 263-268.
3. J. Tuoriniemi, G. Cornelis, M. Hassellöv, M. *Anal. Chem.*, 2012, **84**, 3965-3972.
4. H. E Pace, N. J. Rogers, C. Jarolimek, V.A. Coleman, C. P. Higgins, J. F. Ranville, *Anal. Chem.*, 2011, 83, 9361–9369.
5. J. Tuoriniemi, G. Cornelis, M. Hassellöv, *J. Anal. At. Spectrom.*, 2014, 29, 743-752.
6. F. Laborda, J. Jimenez-Lamana, E. Bolea, J.R. Castillo, *J. Anal. at. spectrom.*, 2013, **28**, 1220-1232.
7. J. Liu, K.E. Murphy, R.I. MacCuspie, M. R. Winchester, *Anal. Chem.*, 2014, **86**, 3405–3414.
8. B. Franze, I Strenge, C. Engelhard, *J. Anal. At. Spectrom.*, 2012, **27**, 1074-1083.
9. M. Hadioui, C. Peyrot , K. J. Wilkinson, *Anal. Chem.*, 2014, **86**, 4668–4674.
10. G. Cornelis, M. Hassellöv, *J. Anal. At. Spectrom.*, 2013, **29**, 134-144.

11. O. Borovinskaya, B. Hattendorf, M. Tanner, S. Gschwind, D. Günther, *J. Anal. At. Spectrom.*, 2013, **28**, 226-233.

12. S. Lee, X. Bi, R.B. Reed, J.F. Ranville, P. Herckes, P. Westerhoff, *Environ. Sci. Technol.* 2014, **48**, 10291–10300.

13. S. Gschwind, L. Flamigni, J. Koch, O. Borovinskaya, S. Groh, K. Niemax, D. Gunther, *J. Anal. at. Spectrom.*, 2011, **26**, 1166-1174.

14. K. Shigeta, H. Traub, U. Panne, A. Okino, L. Rottman, N. Jakubowski, *J. Anal At. Spectrom.*, 2013, **28**, 646-656.

15. N. Jakubowski, L. Moens, F. Vanhaecke, *Spectrochim. Acta B*, 1998, **53**, 1739–1763.

16. A. Hineman, C. Stephan, *J. Anal At. Spectrom.*, 2014, **29**, 1252-1257.

17. M.D. Montaño, H. R. Badiei, S. Bazargan, J.F. Ranville, *Environ. Sci. Nano*, 2014, **1**, 338-346.

18. C. Bouman, M. Deerberg, J. B. Schwieters, Application note: 30187, Thermo Fisher Scientific, Bremen, Germany.

Toc Entry

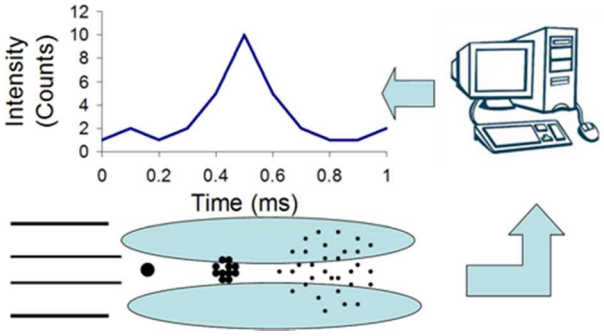

The size detection limit for single particle ICP-MS is improved by rapid data acquisition combined with a new peak recognition algorithm.

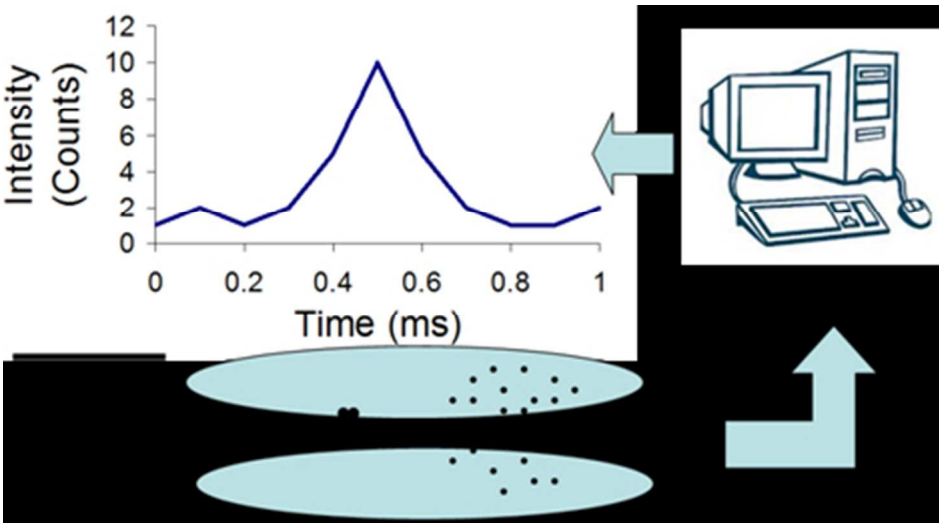

79x43mm (150 x 150 DPI)